AMODE Final Cutoff Travel Times

Brian Dushaw

Applied Physics Laboratory,
College of Ocean and Fishery Sciences,
University of Washington, Seattle, Washington

April 2003

1. Introduction

This is a report describing the derivation of final cutoff travel times from the AMODE acoustic data. An initial attempt at deriving these data was described in the 1996 AMODE data report (Dushaw et al. 1996). The receiving array at each of the moorings consisted of a four-element hydrophone array, with 1.5 wavelength (9 m) spacing of the hydrophones. These hydrophones arrays were located at about 1000 m depth, above the acoustic source. This depth lies above the sound channel axis by about 200 m. Mooring 3 included two additional hydrophones located below the acoustic source; data from these deep hydrophones are not discussed here.

The complete AMODE data set was downloaded *en mass* from the SIO data archives using secure copy:

scp -r aogdb.ucsd.edu:/net/sam5/aog/amode/* .

The data are from moorings 1 through 6, with the data from mooring 5 divided into two sections labelled 5a and 5b. (Mooring 5 failed and was replaced just prior to the MST experiment). The data obtained at each mooring are the receptions from each of the other five sources. There are a total of 30 acoustic paths, or 15 reciprocal acoustic paths. For deriving the final cutoff travel times, the "data files after hadamard processing including demultiplexing and before beamforming" are used [the quote is from the README of the directory]. There are two types of files: *.adf and *.agf files. The *.agf files are "guide" files that list the parameters and filenames of the receptions. For example, the file .../avatar1.hadamard/sn1p_06153.agf lists all the receptions at mooring 1 of transmissions from source 5. This file is used by the FORTRAN programs to read the data files, which are the *.adf files. Each *.adf file contains the data from a single reception, processed for receptions from a single source; there are four complex timeseries (real and imaginary parts) from the four hydrophones.

All travel times are corrected for the motion of the moorings and for clock drift. The program used to make these corrections to the deep-turning rays was used to write out the corrections for zero ray arrival angle. These corrections were applied to the data

prior to processing; it is a simple correction to apply.

2. Processing

The AMODE receptions at each hydrophone are recorded at 2 ms intervals for a sequence spanning an interval of 24.564 s. There are 12282 samples in each reception. Previously, final cutoff travel times were derived from each hydrophone, and then those four travel times were averaged, with attempts to remove those travel times that were obviously outliers. The processing here changes this approach by combining the four travel-time sequences in an rms fashion - this seems to avoid having any outliers to begin with. The combination of the four sequences does not account for an arrival angle, so a zero arrival angle is assumed. In retrospect, this assumption is reasonable, because the latest rays arrive at the reciever depth at near zero arrival angle, i.e., the recievers are near the upper turning depth of the latest arriving rays. The time series used to derive the final cutoff travel time of a particular reception is,

$$T(i) = \sqrt{¼ \sum_{k=1}^{k=4} (h_k^r(i))^2 + (h_k^i(i))^2}$$

where $h_k^r(i)$ and $h_k^i(i)$ are the real and imaginary components of the reception (from which amplitude and phase are derived) at the kth hydrophone. On occasion, one or more of these hydrophones will be particularly noisy, in which case that record will not be used. If the rms noise of an individual hydrophone record is more than twice that of the minimum of snr's for all the hydrophones, it is assumed to be a noisy hydrophone record.

The arrival time of the final peak is first roughly determined to allow that travel time to be bracketed by a few seconds - this avoids having to process the entire 24.564 s (12282 samples) sequence. The root-mean-square of the last 250 samples of the subsequence (a 0.5 s interval) is calculated to estimate a nominal value of the noise. This value sets the scale that is used as the basis for deriving the location of the cutoff.

Starting from the latest travel time and working towards the earlier times, the program first detects sequence values that are three times the value of the noise. To guard against isolated spikes in the sequence, once such a candidate for the location of the cutoff is found, 5 values on either side of that candidate are summed together. The value of that sum must be 5 times larger than the noise to verify that this section of the arrival sequence has substantial acoustic signal. If this criteria is satisfied, the approximate location of the cutoff is assumed to have been found. The program then backs up by 9 samples (i.e., to a time 18 ms later) and, incrementing to earlier times, finds that sample that

increases relative to the later sample (2 ms later) by a value greater than the noise. The time associated with the sample just after this increase is taken as the final cutoff travel time (Figure 1a,b).

One problem arose with processing the data recorded at mooring 2. Recall that the receiver electronics on that mooring had a failing chip causing it to lose integer seconds in travel time (e.g., Dushaw et al. 1996). This apparently is not a problem, so long as the seconds were added back in. It appears that for receiver 2, the data in the hadamard directories is junk for yeardays after about 221 - this is about the time that the travel time shift is supposed to increase to 4 s. I don't claim to understand the details of the data and processing, or that my processing is guaranteed to be correct, but there is a problem getting final cutoff travel times from receiver 2 after yearday 221. It looked as if the data for the receptions after this data (hadamard processed files) were junk. This may not be an issue that I will be able to sort out.

NOTES

(1) There has been no search for, or filtering of, outliers. The results here should be considered a quick and dirty tour through AMODE final cutoff travel times. I think the potential quality of these data are apparent - the various time series are sometimes very encouraging.
(2) The path 6,3 had an odd late peak at about 9.8 s, for which there was no corresponding peak in the path 3,6. Processing was kludged to omit this peak, otherwise differential travel times were unphysically large.
(3) All receptions at mooring 2 end at around yearday 221; apparently the hadamard files are junk after this yearday.
(4) Differential time series with a large offset may suggest that a non-zero arrival angle is present (and not corrected for).
(5) The time series for many of the final cutoff records are considerably longer than the tracked-ray time series. It may be that the earlier arrivals faded out in intensity so that they became untrackable, but retracking some of these is definitely in order.
(6) The data using source 5a is saved for a rainy day - should there be a request to work these data up, it would be a simple matter.
(7) The final cutoff data are stored in files with names such as p_edge.1_2. The "1_2" means that the data are from source 1 to receiver 2. Similarly, p_edge.3_5b contains data from source 3 to receiver 5b. The reciprocal data is given in files such as p_edge.2_1.

3. The Meaning of the Final Cutoff (In this Case...)

Ray tracing for the path from source 2 to receiver 4 predicts that the latest arriving acoustic energy is associated with rays with lower turning depths of 1800–1900 m and

upper turning depths of around 900 m (Figure 17). The source/receiver angles of the cutoff rays are ±3–3.5º. The predicted travel time of these rays is 444.240 s, while the measured cutoff travel times of Figure 1a,b have an absolute travel time of (9.88 + 434.436) = 444.316 (Dushaw et al. 1996), or about 76 ms later. These rays sample well below the maximum of the first baroclinic temperature mode, and they encompass the zero crossing of the first baroclinic current mode (Figure 17). It is therefore not obvious that the final cutoff travel times should show enhanced mode-1 variability in either temperature or current. The sampling of these rays is well below the depths of the main thermocline.

The timefront associated with the above-axis source (Figure 18) is characteristic of an off-axis acoustic source. It is not altogether clear that the source at 1000-m depth would excite the lowest acoustic modes in this case, or if those modes would be detected at the receiver. The 76-ms difference between measured and predicted cutoff travel times is somewhat larger than the travel time variability that is observed, but predictions ought to be made using the hydrographic data obtained during AMODE. A delay in the observed finalé relative to the ray prediction may be suggestive of excitation of slower modes. It appears from the figure that the actual receptions have a large peak towards the end of the reception that might be identified with the final arrival in the ray prediction, followed by some additional acoustic energy before the final cutoff. More work is required to fully understand this particular issue.

The tidal variability is frequently consistent with the sum and difference data of the ordinary rays. There is a suggestion that tidal currents observed by differential travel times in the northern part of the array are large, perhaps a signal of the resonant diurnal internal waves. (Are these signal diurnal?) However, the timeseries appear to be fairly noisy; a more careful derivation of final cutoff travel times is probably required before any conclusions can be drawn. Other than to say that the tides in the cutoff travel times are consistent with the ordinary ray travel times, there is not much new that the final cutoff travel times bring to this issue (at least nothing obvious).

The final cutoffs derived from the RTE87 data were associated with receivers that were located near the depths of the sound channel axis. These travel times are therefore perhaps best associated with the travel time and sampling of the gravest acoustic mode. The receivers of AMODE were off the sound channel axis by 200 m or more. Experiments such as SLICE’89 show that acoustic energy "diffuses" away from the sound channel axis near the finalé. The temporal variability of this "diffusion" is unknown, as is the actual spatial sampling of the "diffused" energy. These complications are obviously relevant to interpretation of the AMODE cutoff travel times. There are as yet no answers to questions such as these. It seems obvious, therefore, that, as useful as these travel times may be, they ought to be approached with a degree of suspicion.

REFERENCE

Dushaw, B. D., P. F. Worcester, B. D. Cornuelle, A. R. Marshall, B. M. Howe, S. Leach, J. A. Mercer, and R. C. Spindel, 1996: Data report: Acoustic Mid-Ocean Dynamics Experiment (AMODE). APL-UW TM 2-96. Applied Physics Laboratory, University of Washington, Seattle, Washington, 275 pp.
http://faculty.washington.edu/dushaw/epubs/Dushaw_AMODE_Data.pdf

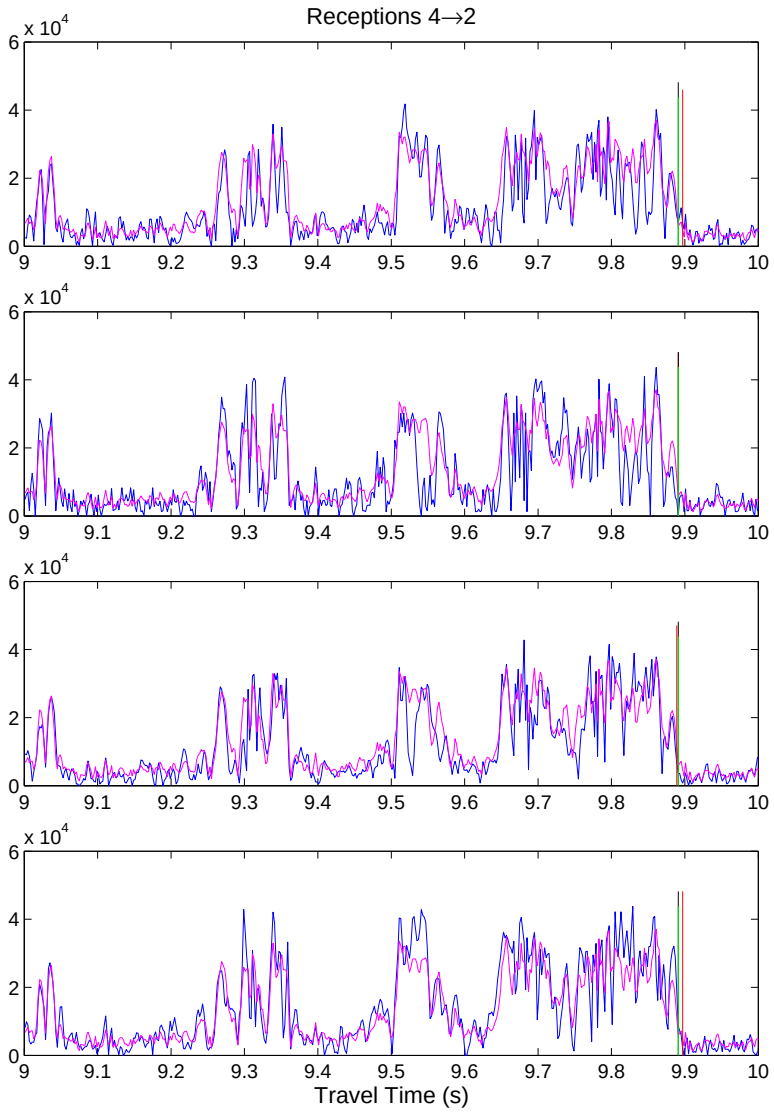

Figure 1a. An example of a reception at mooring 4 from source 2 transmissions. Each panel shows the reception at each hydrophone as the blue curve. The units of the ordinate are amplitude on a linear scale. The magenta curve shows the root-mean-square average of the four receptions used to obtain the final cutoff travel time; the magenta curves in each panel are identical. Green vertical bars show a previous estimate of final cutoff travel times. Red vertical bars show a recent estimate of the cutoff for each hydrophone reception. The black vertical bar shows the cutoff travel time based on the procedure outlined in the text. The full reception spans 0–24.564 s. The instability of the shape of this later part of the arrival pattern and lack of a definitive last large-amplitude pulse are evident. Like snowflakes, each reception is unique.

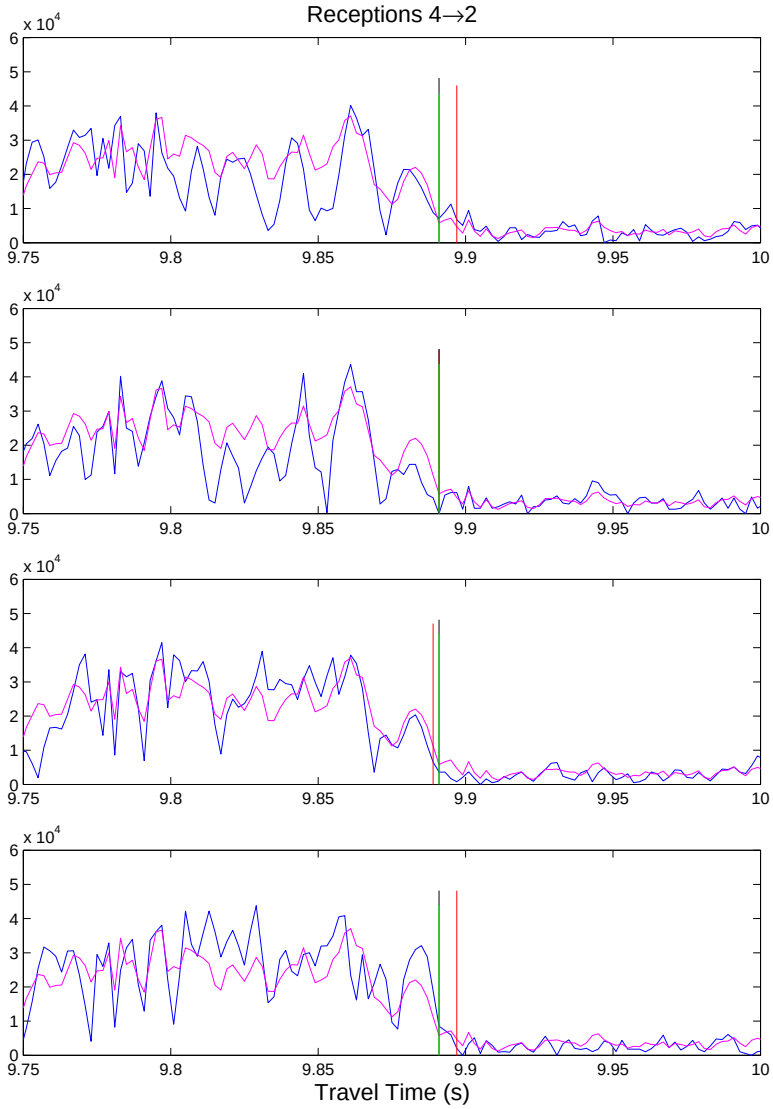

Figure 1b. Close-up of the finalé.

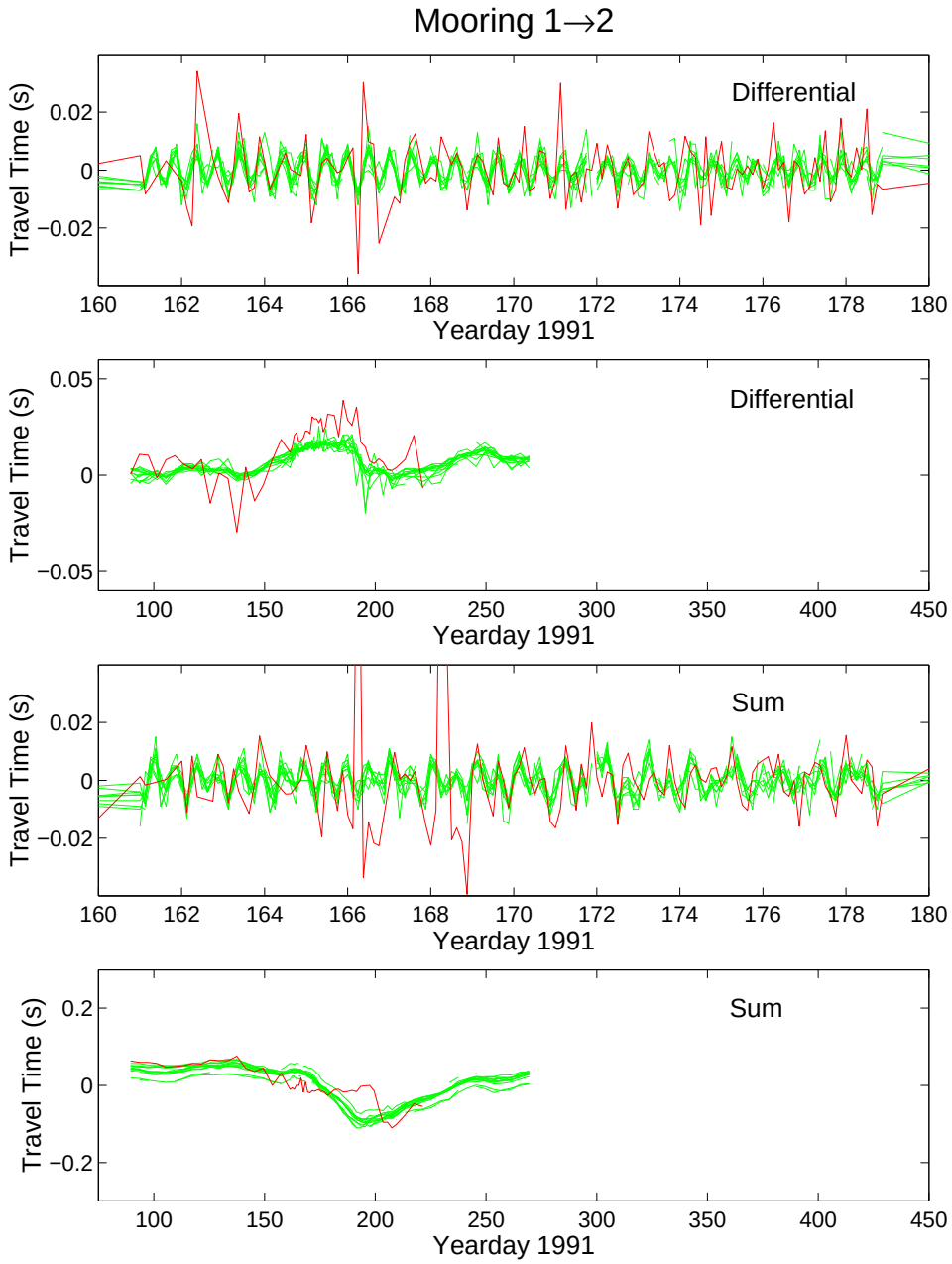

Figure 2. Differential and sum travel times from path 1,2. As for figure 3.

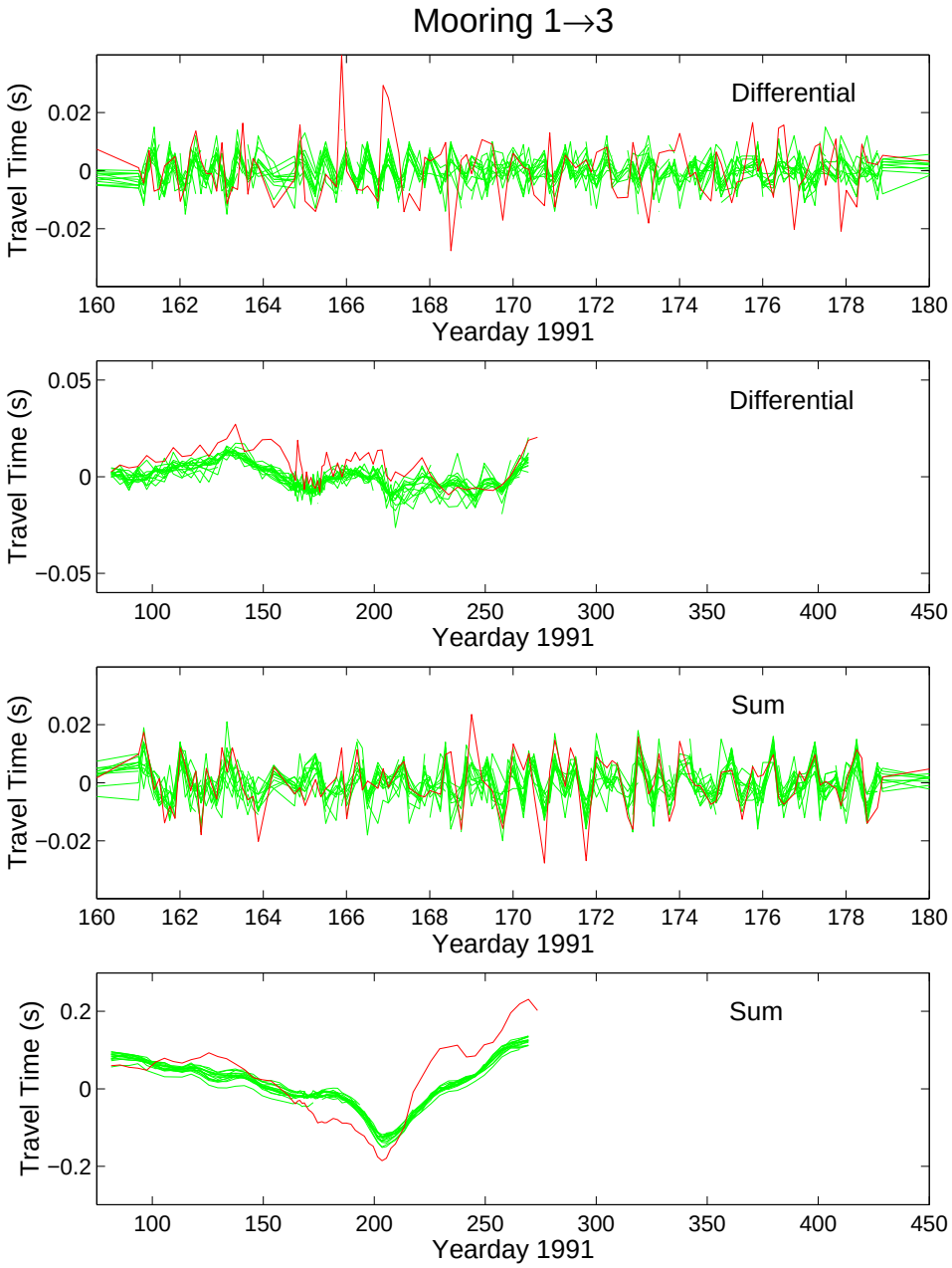

Figure 3. Differential and sum travel times from path 1,3. As for figure 2.

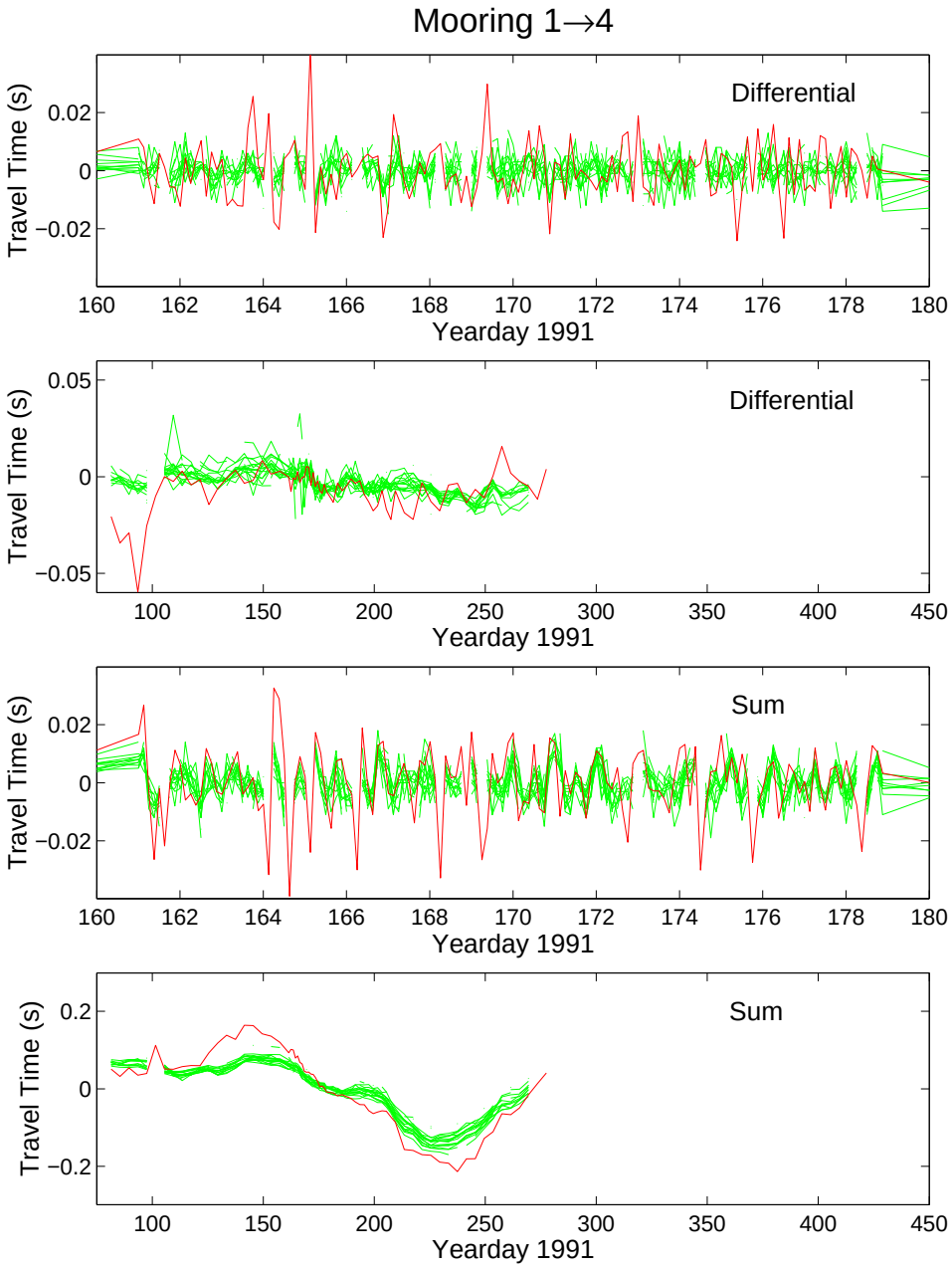

Figure 4. Differential and sum travel times from path 1,4. As for figure 2.

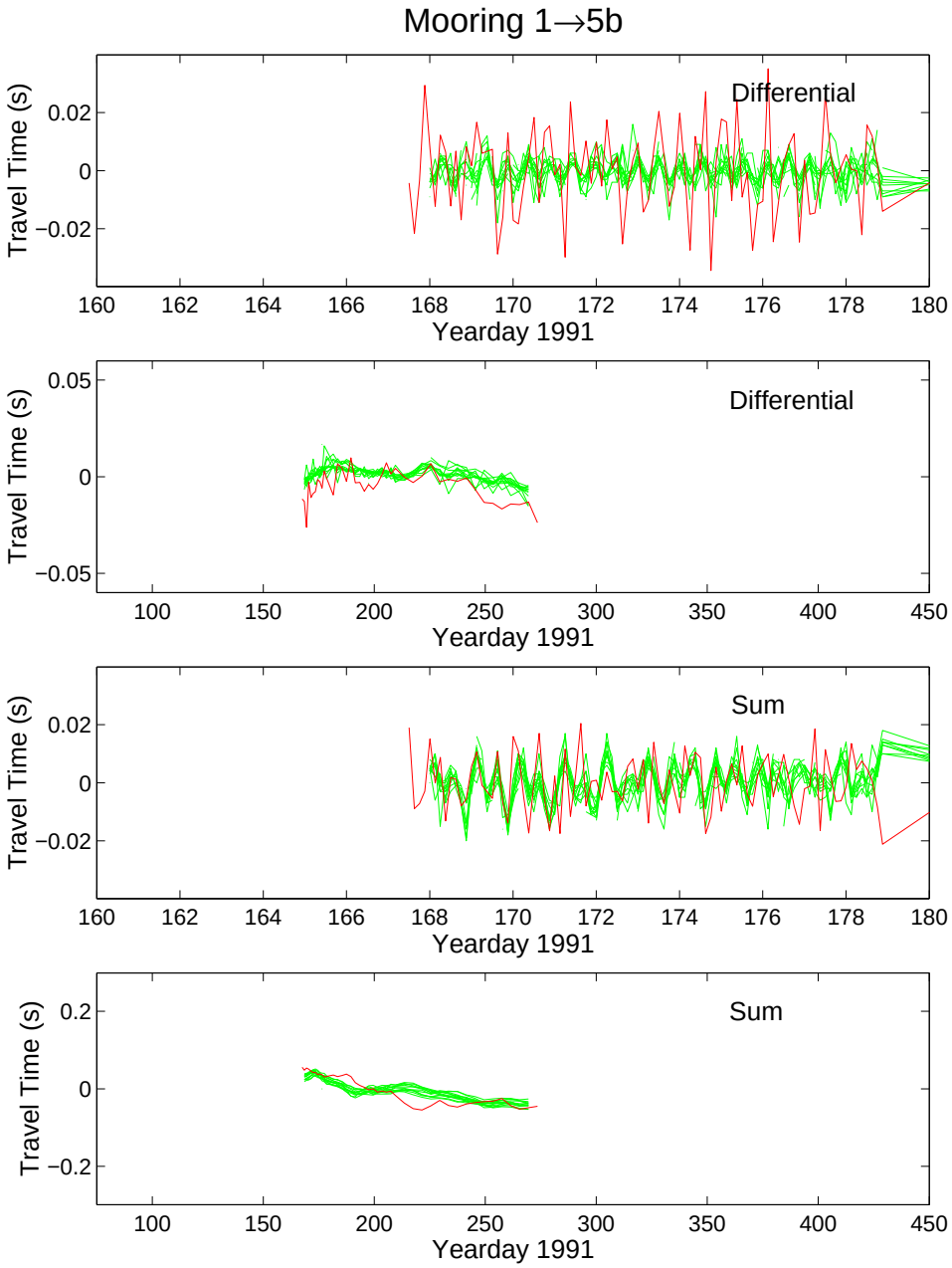

Figure 5. Differential and sum travel times from path 1,5b. As for figure 2.

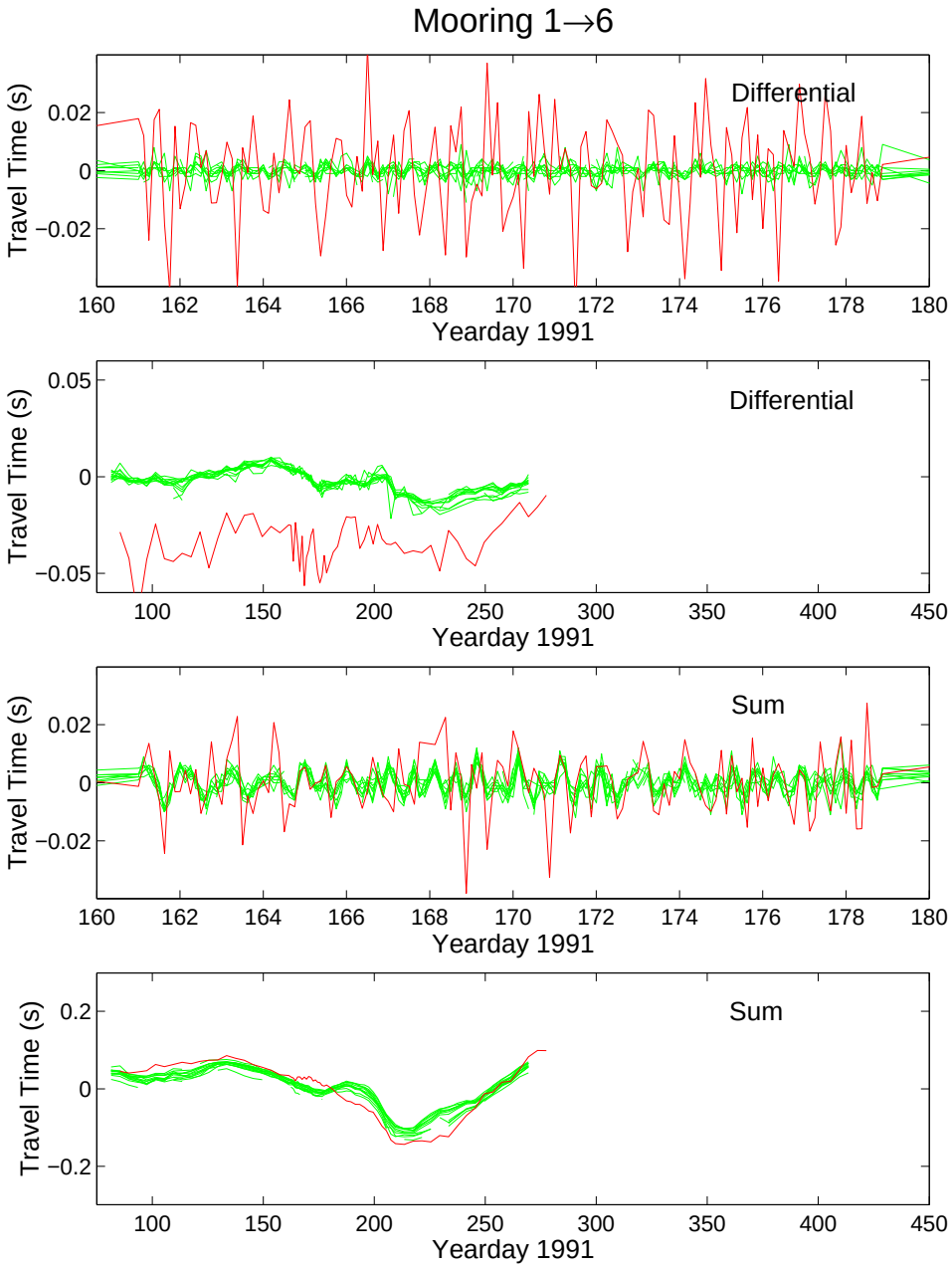

Figure 6. Differential and sum travel times from path 1,6. As for figure 2.

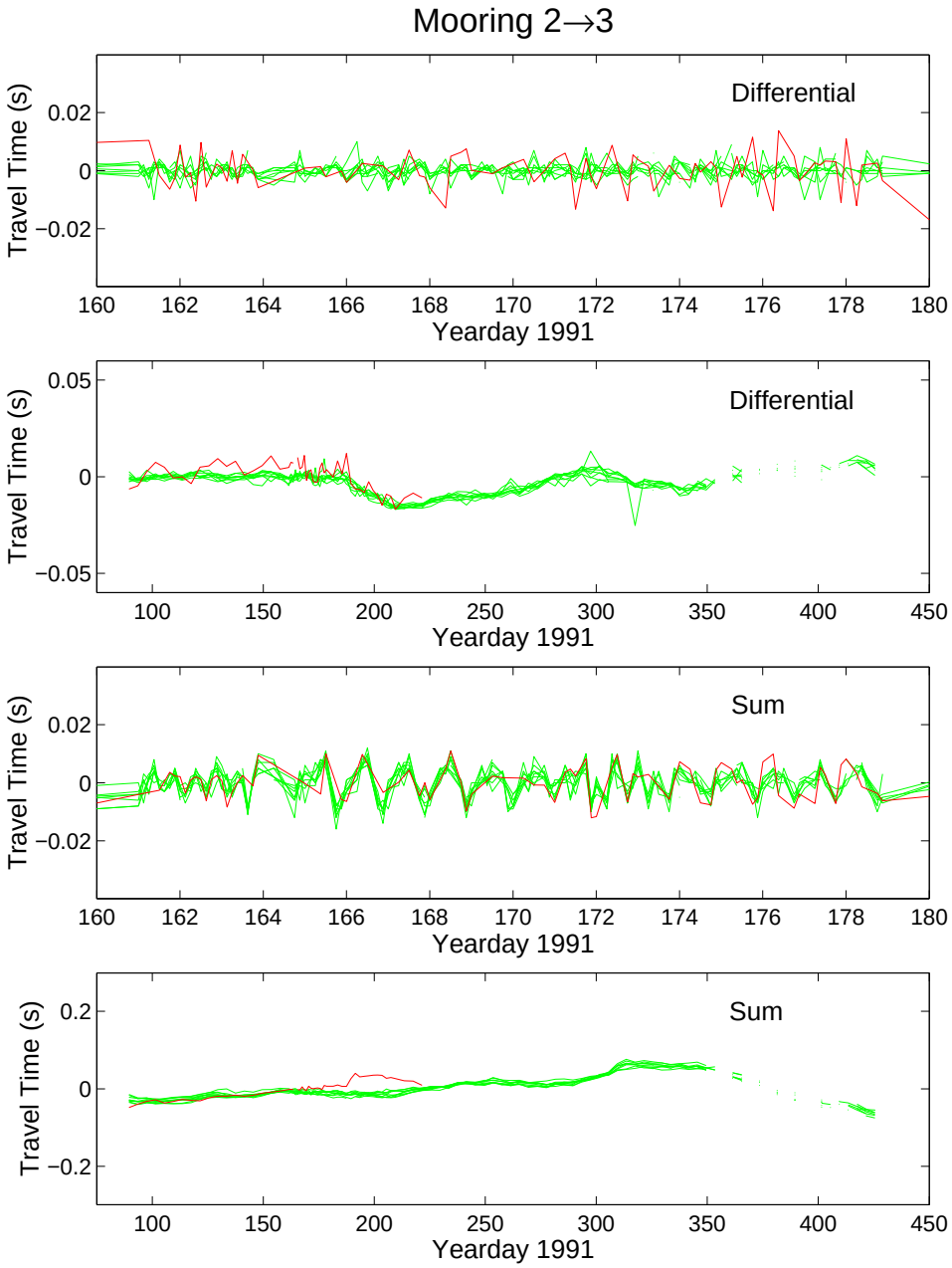

Figure 7. Differential and sum travel times from path 2,3. As for figure 2.

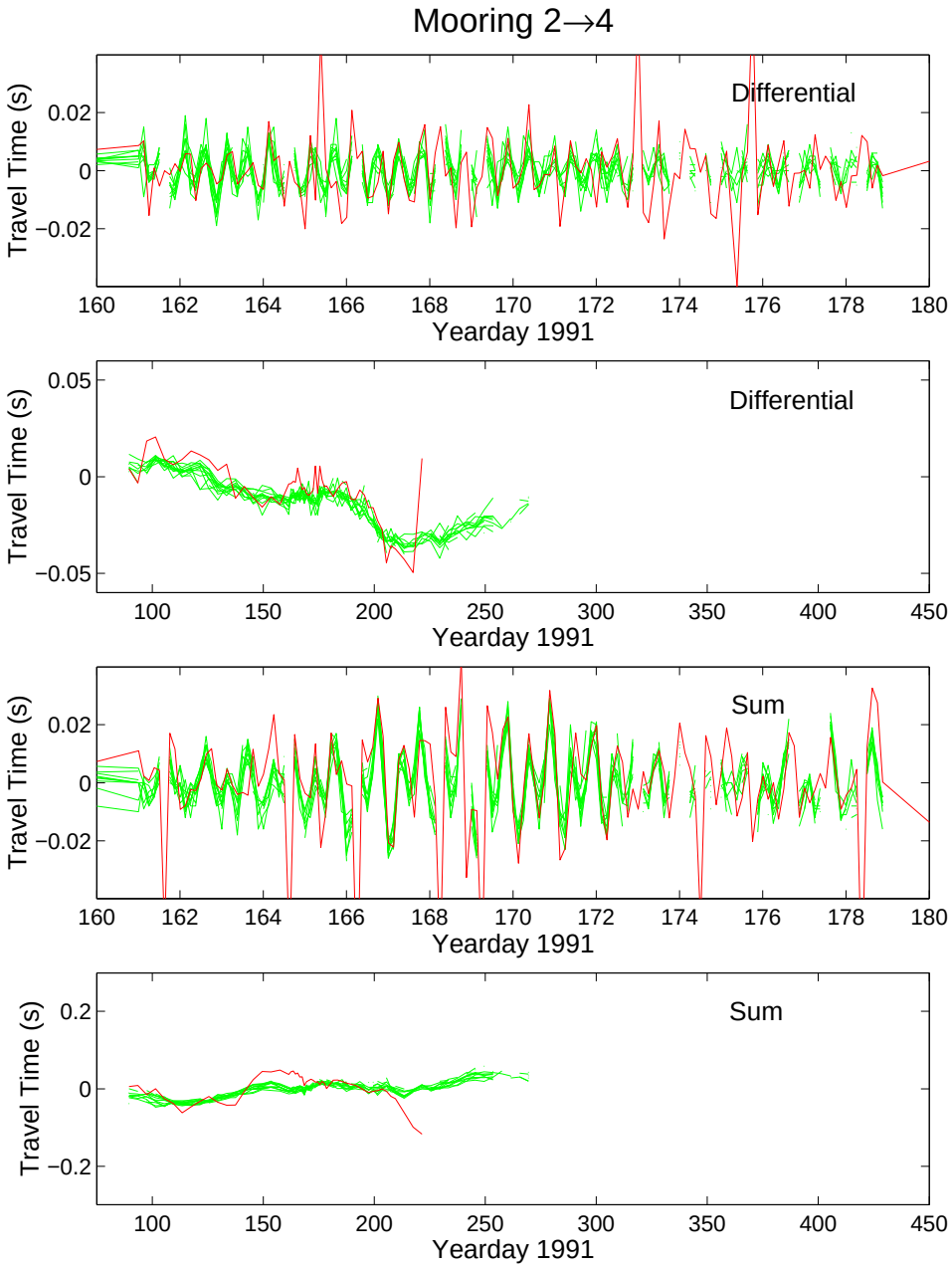

Figure 8. Differential and sum travel times from path 2,4. As for figure 2.

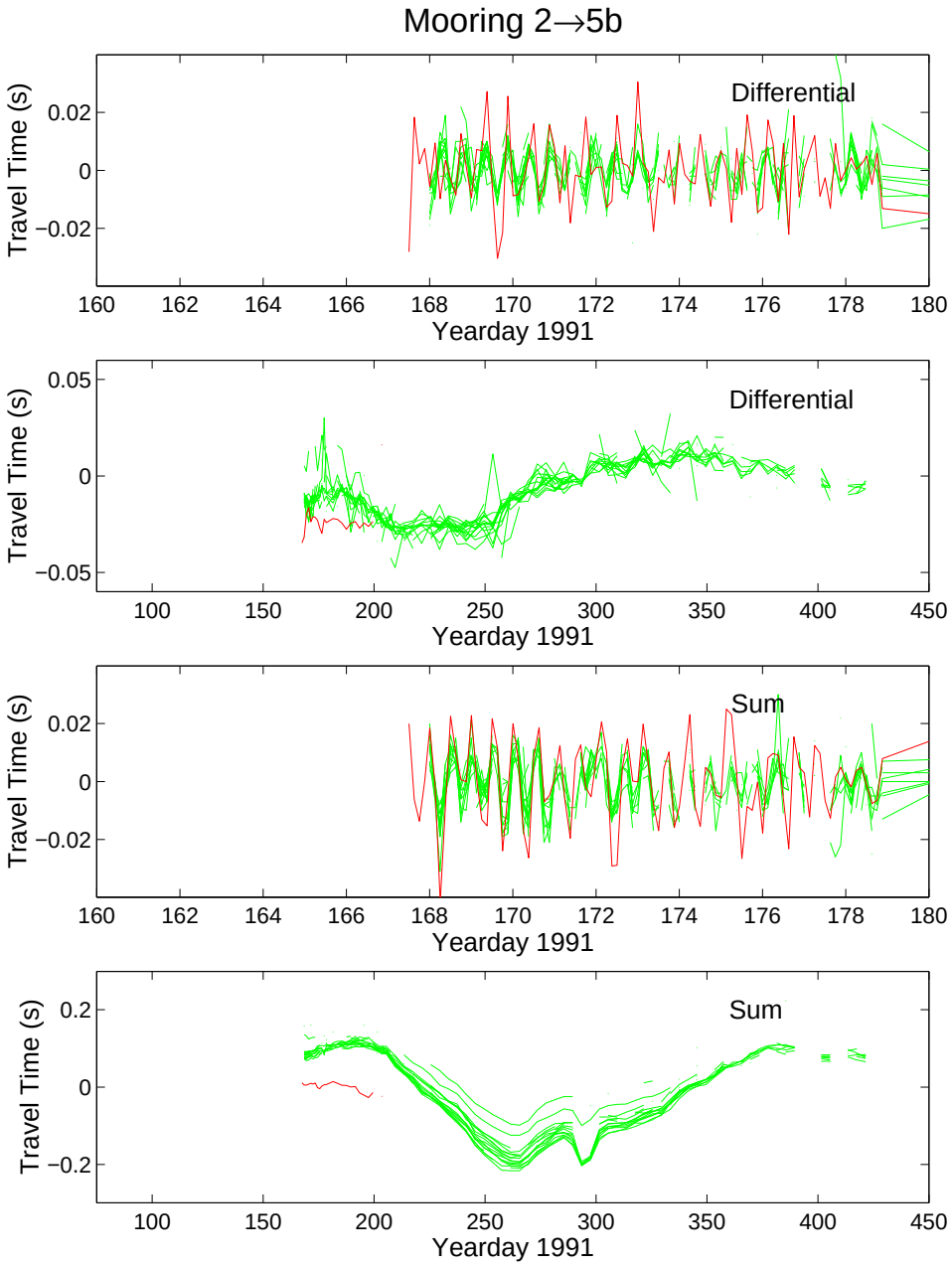

Figure 9. Differential and sum travel times from path 2,5b. As for figure 2.

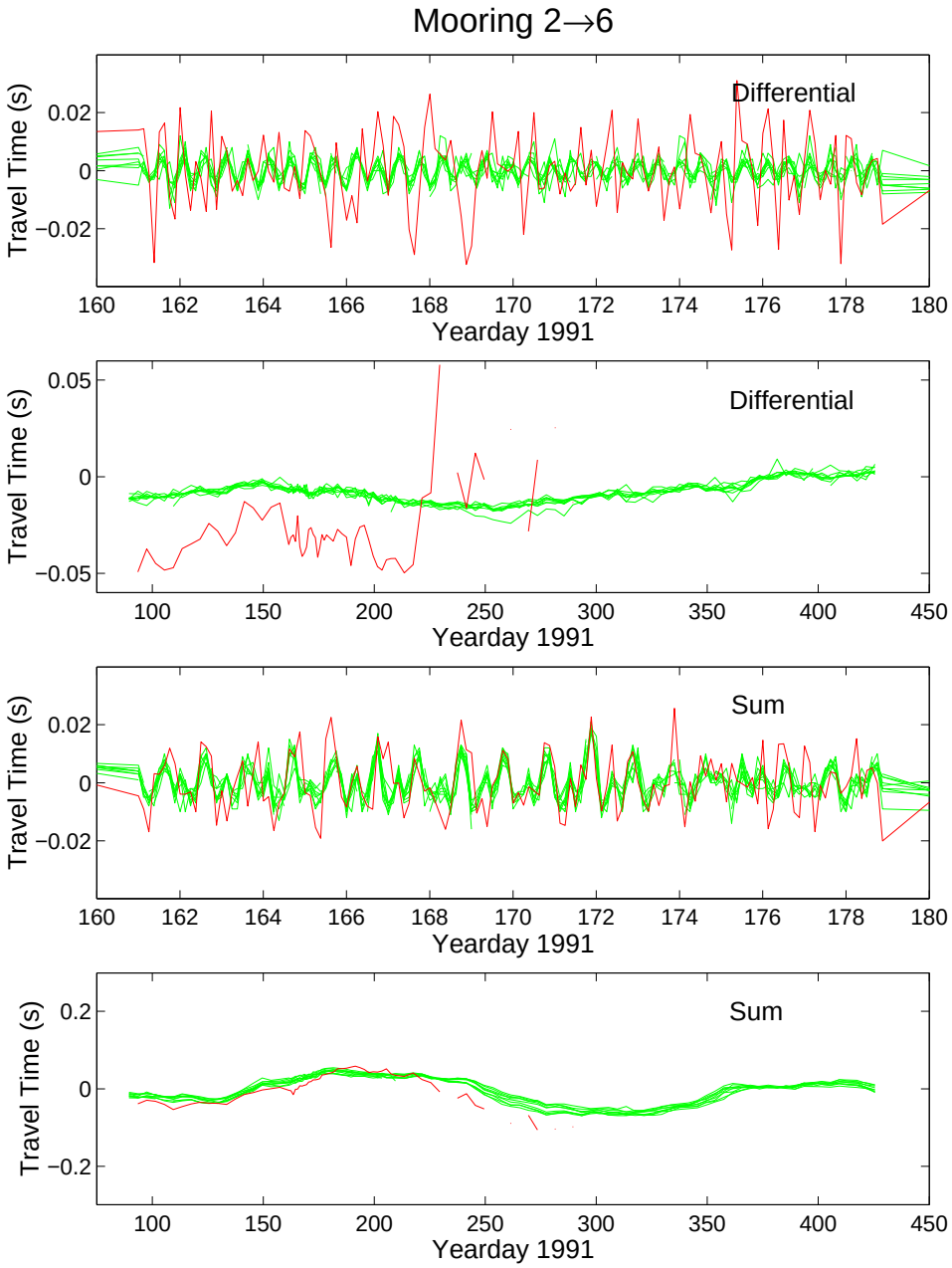

Figure 10. Differential and sum travel times from path 2,6. As for figure 2.

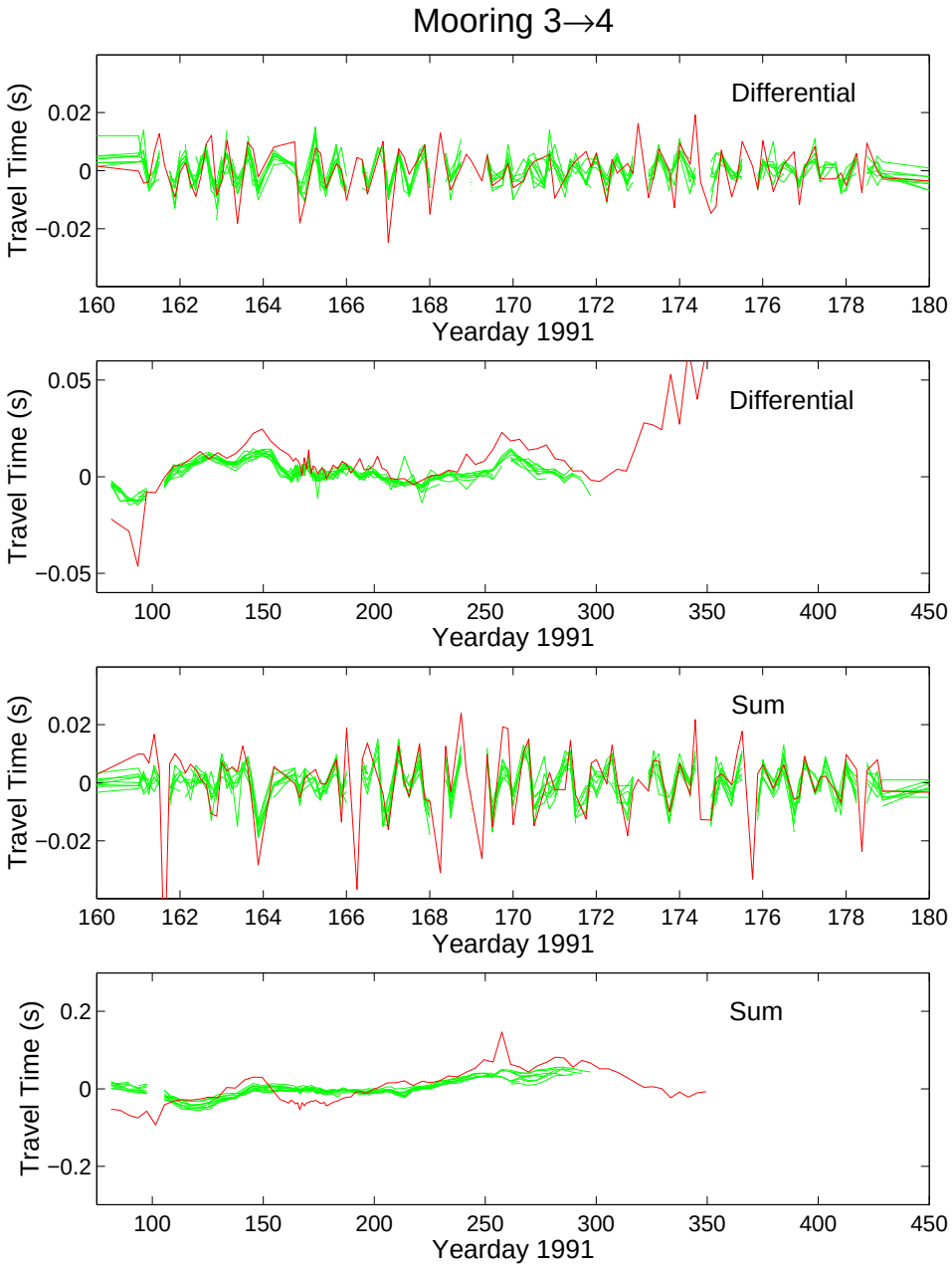

Figure 11. Differential and sum travel times from path 3,4 As for figure 2.

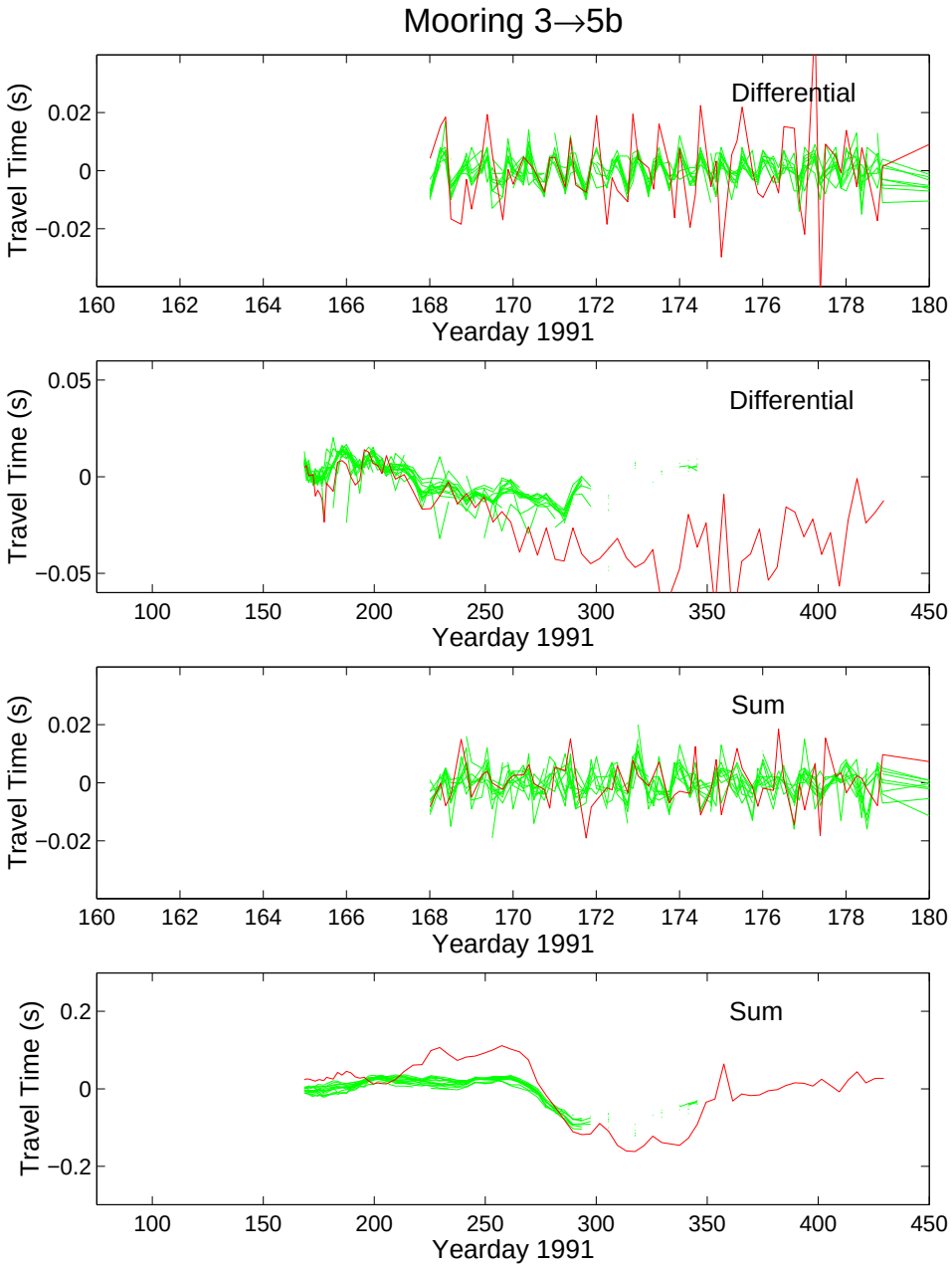

Figure 12. Differential and sum travel times from path 3,5b. As for figure 2.

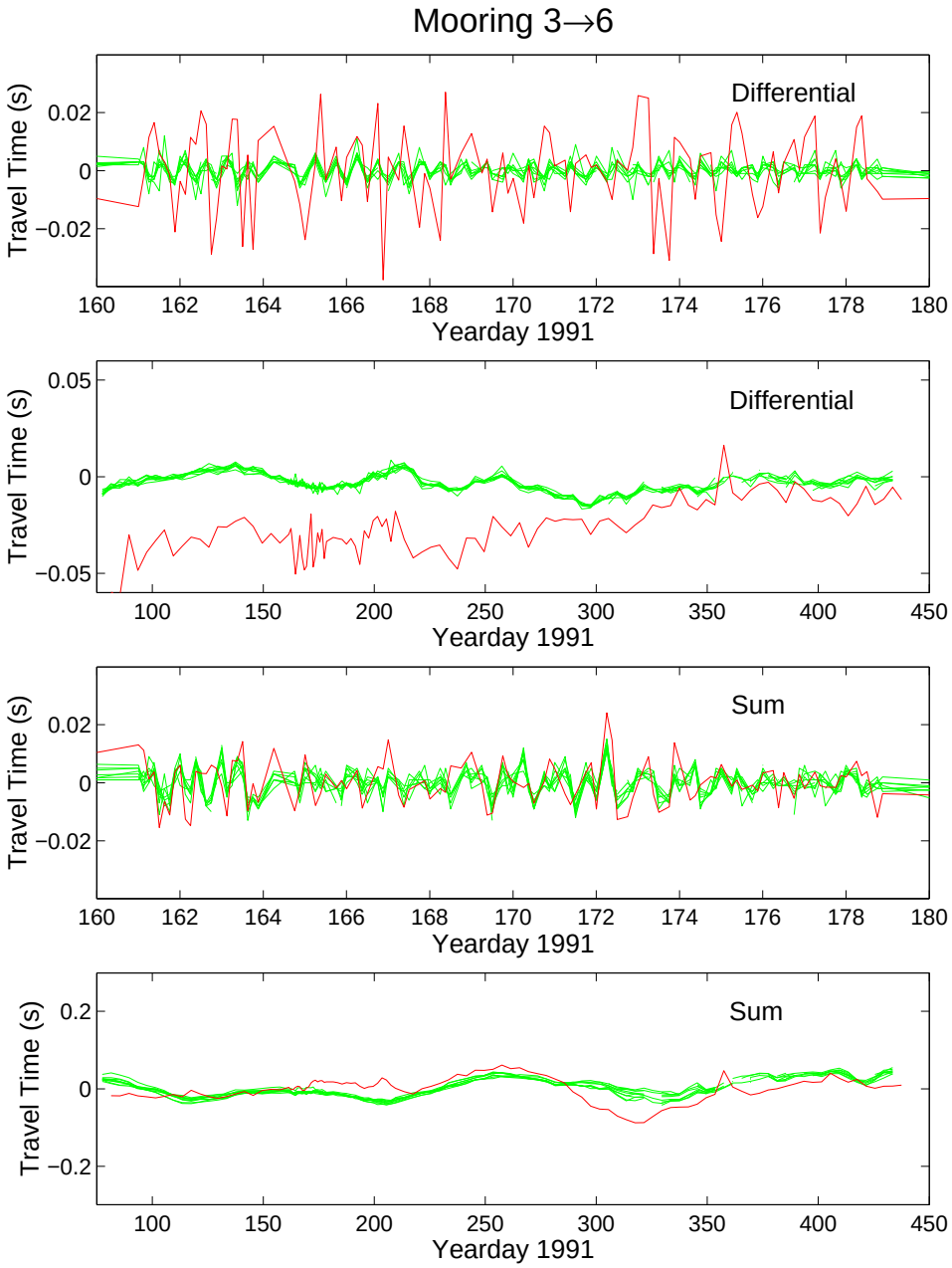

Figure 13. Differential and sum travel times from path 3,6. As for figure 2.

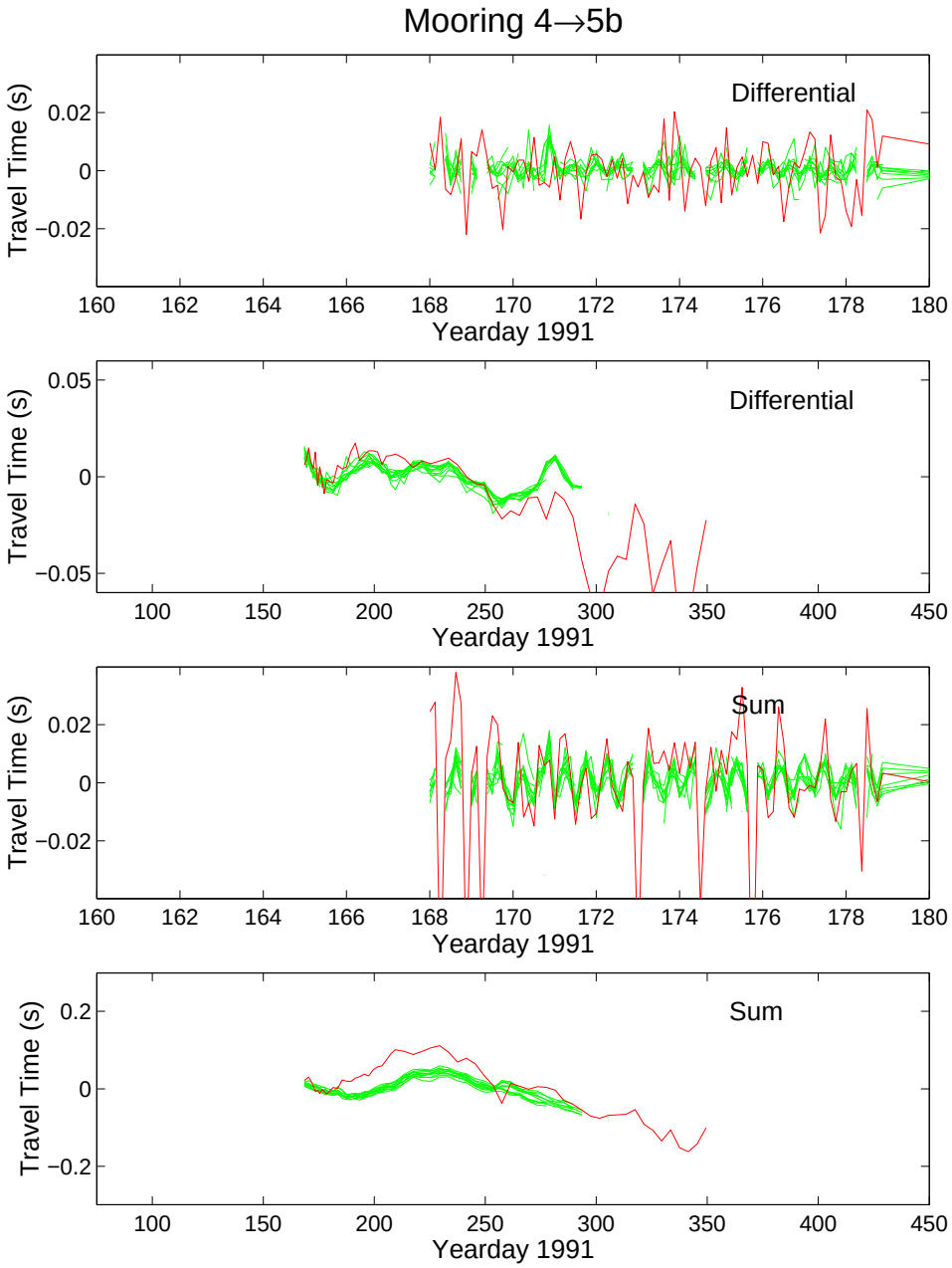

Figure 14. Differential and sum travel times from path 4,5b. As for figure 2.

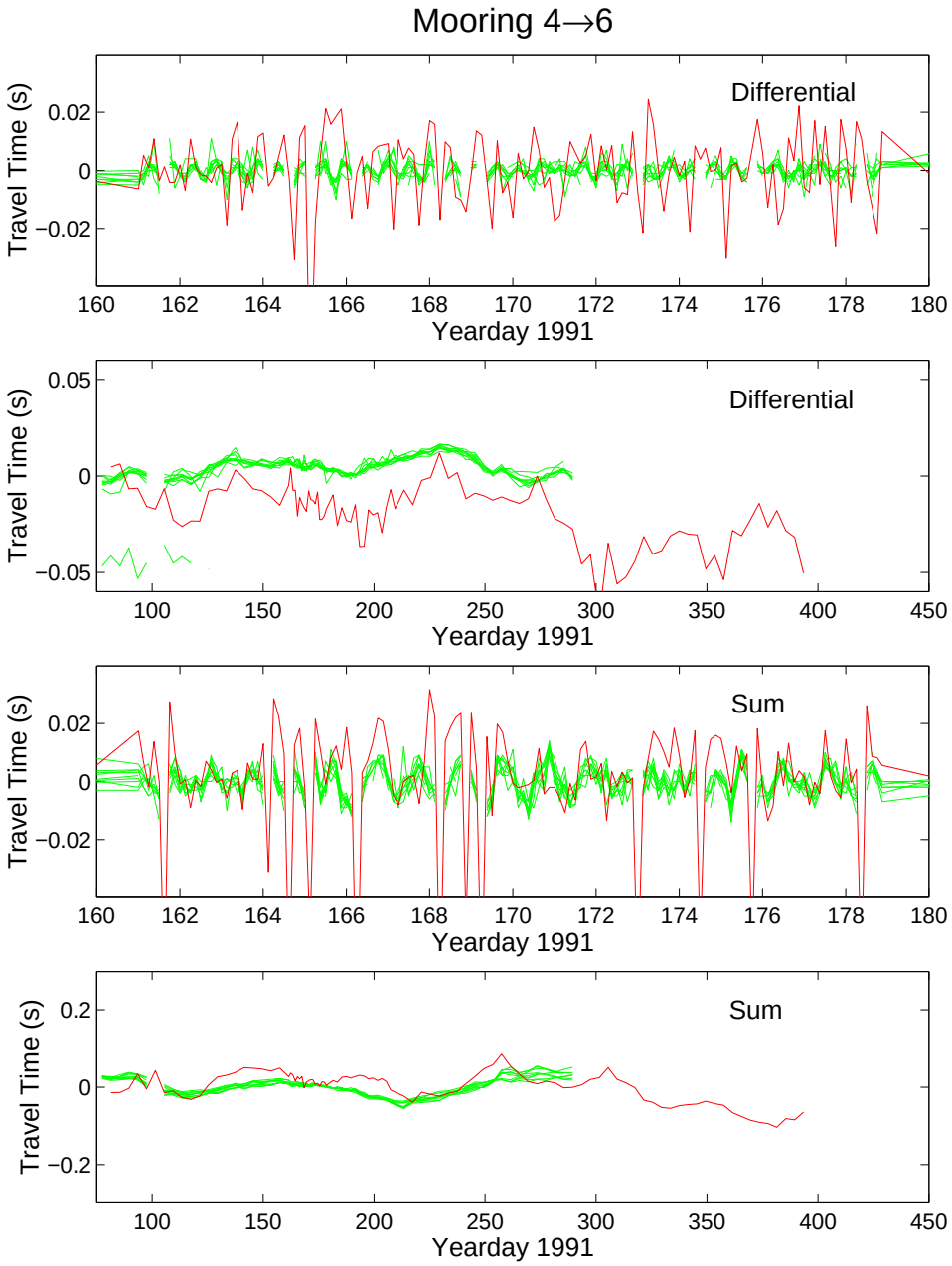

Figure 15. Differential and sum travel times from path 4,6. As for figure 2.

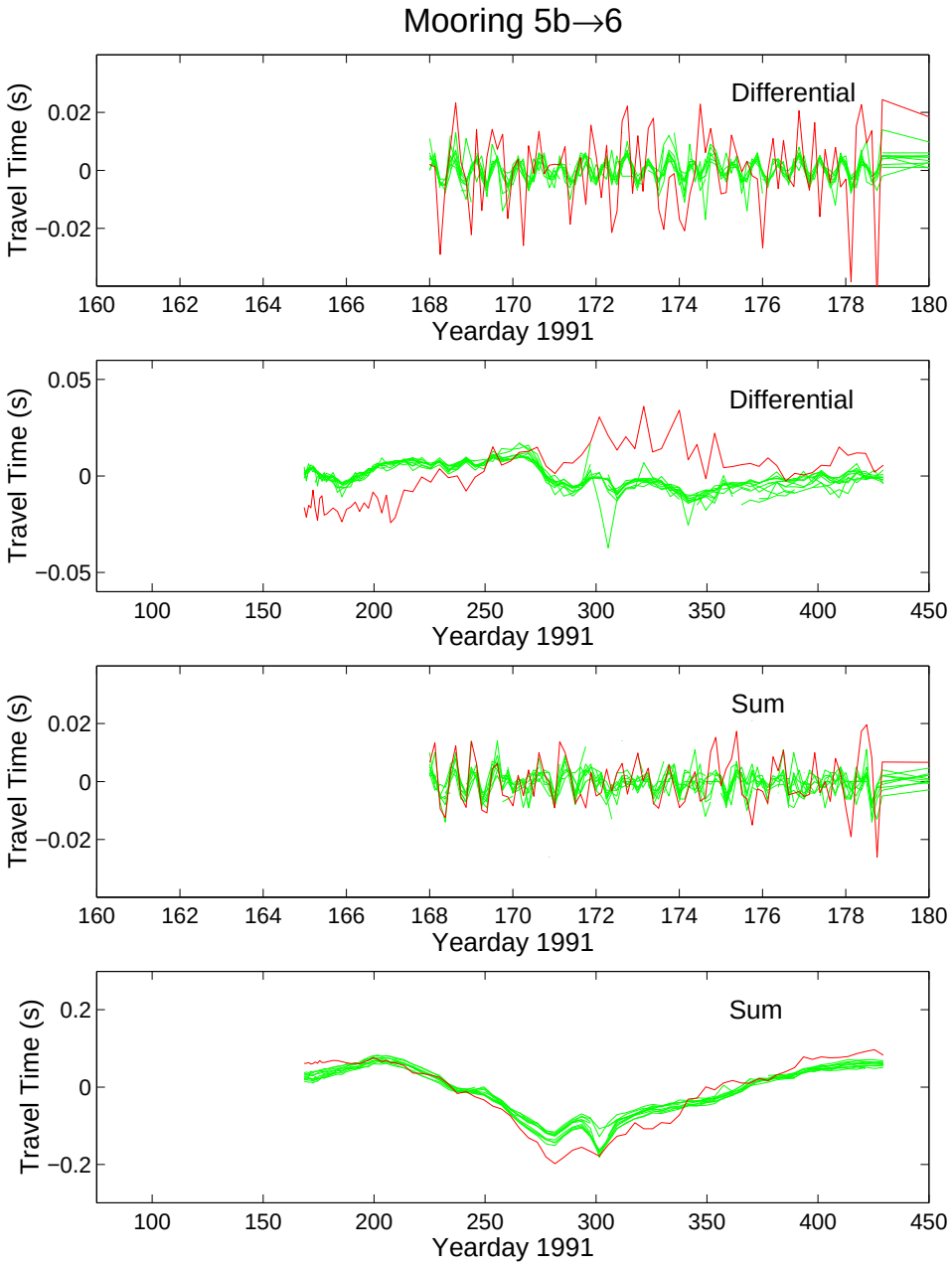

Figure 16. Differential and sum travel times from path 5b,6. As for figure 2.

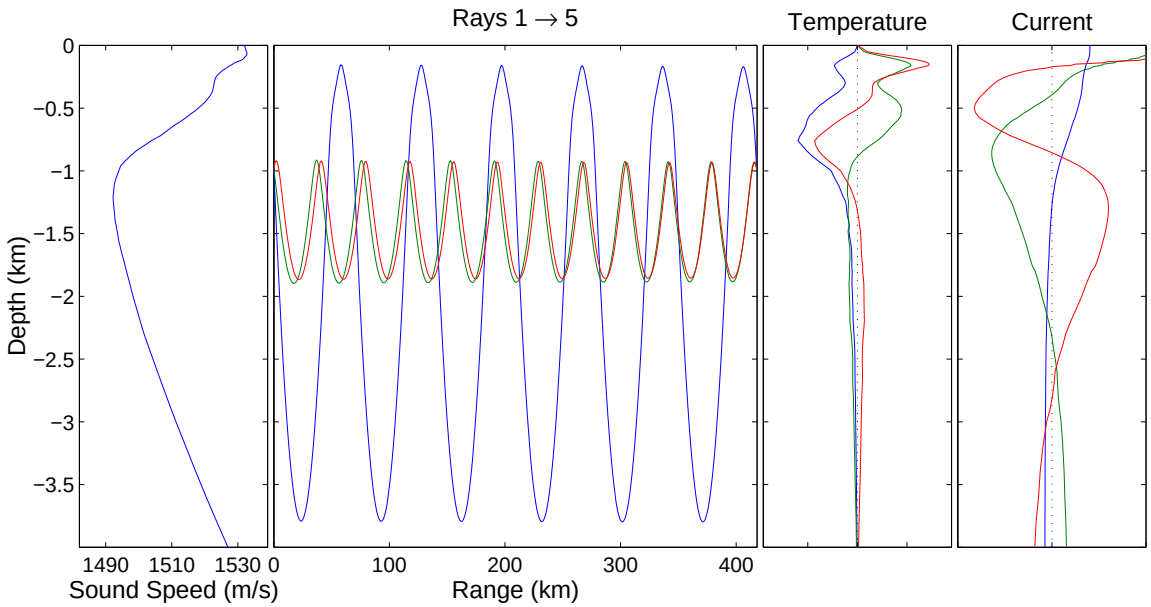

Figure 17. Sound speed profile, rays, temperature modes and current modes. The rays are derived from path 2,4, and only a nominal deep-turning ray and a pair of "final cutoff" rays are shown. The ray sampling is below the depths where the mode-1 temperature is largest, and the rays span the depth of the zero crossing of mode-1 current.

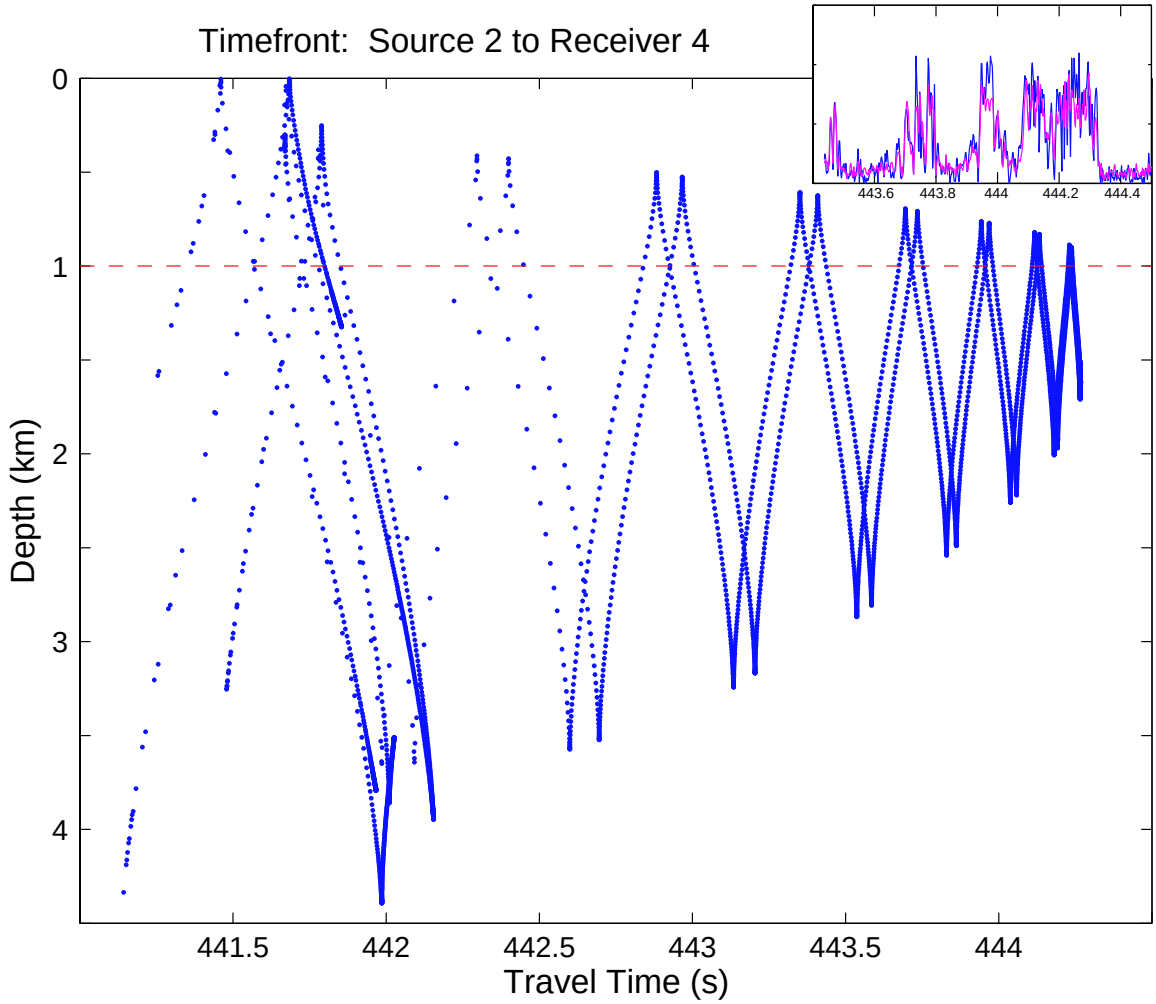

Figure 18. Predicted timefront for the path from source 2 to receiver 4. The depth of the receiver is shown by the dashed red line. The latest travel time at this depth is about 444.24 s. The predictions show a pattern that suggests the last ray arrival should be resolvable in the data, but the recorded finalé is hardly so clear. The arrival pattern in the inset is that of the lower panel of Fig. 1a.